

Optimisation of an Inertial Mechanism within a Uni-Axial Vibration Isolator to Suppress Internal Resonance

Paul Dylejko

Maritime Platforms Division, Defence Science and Technology Organisation, Fishermans Bend VIC 3207, Australia

ABSTRACT

Internal resonances within vibration isolators have been shown to increase force transmissibility and radiated noise from supporting structures. This paper theoretically investigates the optimal use of an inertial mechanism within a uni-axial vibration isolator to reduce the influence of these internal resonances. The inertial mechanism under consideration is associated with a device which exerts an inertial force proportional to the relative acceleration of its connection points. Examples of such devices include dynamic antiresonant vibration isolators, resonance changers and inerters. It has been shown that these devices can be used to establish suppression bands in vibration transmission. Previous research has examined the use of such a device for attenuating low frequency vibration transmission. This work considers the inertia of the isolator and minimises the force transmissibility over a wider frequency range to include the effect of internal resonances. The optimisation is carried out using a combination of a particle swarm and gradient based optimisation algorithm. It is shown that this isolator configuration has the potential to reduce the force transmissibility to levels approaching an ideal vibration isolator over a wide frequency range.

INTRODUCTION

Resilient elements are commonly used to reduce the transmission of vibrations from machinery to supporting structures. This form of control represents a manipulation of the transmission path. Vibration isolators reduce transmitted vibration by dissipating or impeding the transfer of vibrational energy. Vibration isolation mounts for machinery are typically made of rubber or other viscoelastic materials, although steel springs can also be used. The theory on isolation is well understood (Beranek et al., 1992, Harris, 1995). The performance of an isolator can be characterised by the ratio of transmitted force to the excitation force. This ratio is commonly referred to as the force transmissibility. Isolation systems are frequently analytically modelled at low frequencies as simple lumped-parameter systems with the isolators represented by a complex stiffness. In a recent paper, Moore (2011) used this approximation to study single, two-stage and two-stage rafted isolation configurations. This lumped-parameter approximation which considers the vibration isolator to be massless, however, over-predicts the reduction in force transmissibility at high frequencies.

Real isolators suffer from internal resonances also known as wave effects. These are due to their distributed mass and elasticity. The frequencies of these resonances are related to the material properties and geometry of the isolator, generally occurring in the audible frequency range (Harrison et al., 1952). Sykes (1960) reported that the effectiveness of typical rubber and neoprene vibration isolators was reduced by as much as 20 or 30 dB by internal resonance. Harrison et al. (1952) presented a theoretical and experimental study of internal resonances. A reduction in predicted performance of up to 20 dB for isolators made from various materials was observed. The theoretical study approximated the isolator as a slender elastic rod in longitudinal vibration. It was noted that the theoretical predictions correlated well with the measured results. Snowdon (1979) also approximated the response of isolators as slender longitudinal rods of uniform cross section to examine the influence of internal resonances. It

was commented that for isolators with significant lateral dimensions, a correction to this description can be applied.

Little work has been completed on attenuating internal resonances; this is largely due to the assumption that the transmissibility is already quite low at these higher frequencies. Du et al. (2003), however, showed that they can contribute significantly to the radiated sound power from a supporting structure. This contribution was shown to be an increase of 2 – 22 dB over a 200 Hz – 3 kHz frequency band. The model considered in Du's work was a primary mass with three degrees-of-freedom (bounce, pitch and roll) supported by three isolators on a simply supported rectangular plate in an infinite baffle. Du et al. (2005) later developed a vibration isolator that included two active dynamic vibration absorbers (DVAs) to control internal resonances. The passive properties of the DVAs were optimised to minimise the force transmissibility over two frequency bands. Experiments demonstrated a reduction in force transmissibility up to 20 dB and a 4.3 dB reduction in total acoustic power using the DVAs as passive devices. With active control, the RMS force transmissibility and acoustic power were reduced by 22 dB and 9.1 dB respectively. The importance of internal resonances on active isolation systems was investigated by Yan et al. (2010) who demonstrated velocity feedback was unable to suppress them. Furthermore, it was shown that the internal resonances caused stability issues in the control system.

This paper investigates the potential for mitigating internal resonance using an inertial device which produces a force which is proportional to relative acceleration. An example of such a device is a resonance changer. The inertial force in this device is generated hydraulically by a piston, pipe, and reservoir arrangement. Resonance changers have been used to minimise the vibration transmission in marine propulsion systems (Dylejko et al., 2007). A recent example of a mechanical device was developed by Smith (2002) which utilised a rack and pinion to generate an inertial force proportional to relative motion. This mechanism, known as an inerter, has been successfully used in Formula One cars to reduce tyre load fluctuations. An earlier example of a mechani-

cal device for vibration isolation was proposed by Flannely (1967) and is shown in Figure 1. This device, known as a dynamic vibration antiresonant isolator (DAVI), consists of a levered mass m_{DAVI} in parallel with a stiffness k . Antiresonance occurs when the spring force cancels with the inertial force associated with the levered mass. The leverage can provide inertial amplification resulting in a larger effective mass. This device has been used in the aerospace industry where there are stiffness and mass restrictions on isolators (McGuire, 2003, Smith et al., 2002, Desjardins and Hooper, 1978).

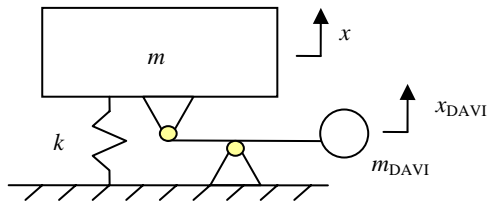


Figure 1. Dynamic vibration antiresonant isolator (DAVI) proposed by Flannely, (1967).

Work by Yilmaz and Kikuchi (2005) demonstrated that multiple DAVIs could be used to establish suppression bands in low frequency force transmission. It was shown that the suppression bandwidth was significantly larger than an equivalent system with a DVA. The suppression bands established by a similar inertial mechanism in finite lattices was investigated by Yilmaz and Hulbert (2010). These suppression bands were compared with band gaps established by local resonance and Bragg Gaps.

The aim of this paper is to theoretically investigate the merit of a symmetrical inertial mechanism for reducing the influence of internal resonances on the force transmissibility of a vibration isolator. For brevity, the inertial mechanism will be referred to from this point as a DAVI. The system modelled in this paper is based on the work completed by Du et al. (2005). This consists of a primary mass supported by a resilient element with two intermediate masses incorporating DVAs. An isolator with intermediate masses is also known as a compound isolator.

Figure 2 shows a graphical representation of the system under consideration in this paper, including a potential implementation of the DAVI in grey. This potential DAVI implementation consists of hinged rods. The inertial force is associated with the rods accelerating laterally with the relative motion of the attached masses. Several elements could be used around the circumference of the isolator to make up the required effective mass. It should be noted that the elastic response of the DAVI is not considered in this preliminary study.

A dynamic model of the vibration isolator supporting a primary mass under uni-axial loading is developed using the transmission matrix approach (Rubin, 1967). Transmission matrices linearly relate the force and velocity at an input to the force and velocity at an output. This sub-structure modelling technique allows for flexibility with future design modifications. The matrices can be determined analytically, computationally or experimentally (Dickens, 1999). The transmission matrices are related to other immittance descriptions such as impedance through matrix transformations (Rubin, 1967).

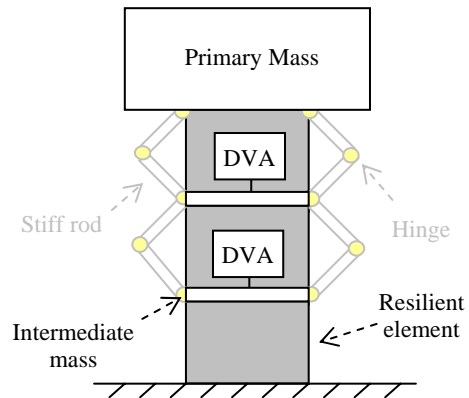


Figure 2. Representation of the vibration isolator considered.

The resilient elements are modelled as continuous rods in longitudinal vibration while the other elements are treated as lumped parameters. Isolator design parameters are chosen by minimising the force transmissibility relative to an ideal isolator over a chosen frequency range. The optimisation is carried out with a particle swarm and gradient based optimisation algorithm. Two isolator configurations are examined: an isolator with two passive DVAs, and one with two DAVIs. The performance of each is compared and their relative merit discussed. Finally, the sensitivity of the force transmissibility to variations in the optimum design parameters is investigated.

ANALYTICAL MODEL OF A VIBRATION ISOLATOR

Sub-structure model

A schematic diagram of the transmission matrix representation of the dynamic system is presented in Figure 3.

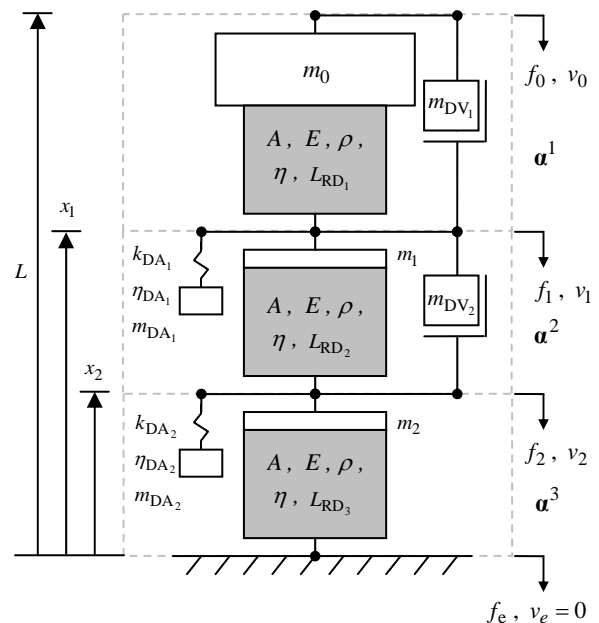


Figure 3. Schematic of transmission matrix model of the vibration isolator.

The velocities of the primary mass m_0 , first intermediate mass m_1 and second intermediate mass m_2 are described by v_0 , v_1 and v_2 respectively. The forces at these locations are given by f_0 , f_1 and f_2 . The first and second DAVI have effective masses of m_{DV_1} and m_{DV_2} respectively. The mass, stiffness and structural loss values for the first and second DVA are described by m_{DA_1} , k_{DA_1} , η_{DA_1} , m_{DA_2} , k_{DA_2} and η_{DA_2} respectively. The resilient elements are assumed to have the same cross sectional area A , Young's modulus E , density ρ and structural loss factor η . The individual lengths of the first, second and third resilient elements are described by L_{RD_1} , L_{RD_2} and L_{RD_3} . The coordinates to the first and second intermediate masses from the bottom of the isolator are given by x_1 and x_2 . The overall height of the isolator is L . The dynamic responses of the individual stages of the compound isolator are described by the transmission matrices α^1 , α^2 and α^3 .

Transmission matrices

In the following, the time dependence of force and velocity is proportional to $e^{-j\omega t}$, where $j = \sqrt{-1}$, ω is the radian frequency and t is time. The transmission matrices for the individual stages are developed from the individual components. The transmission matrices for the n^{th} lumped mass, DVA and DAVI are given by (Snowdon, 1971, Dylejko et al., 2007):

$$\alpha^{M_n} = \begin{bmatrix} 1 & -j\omega m_n \\ 0 & 1 \end{bmatrix} \quad (1)$$

$$\alpha^{DA_n} = \begin{bmatrix} 1 & \frac{-j\omega k_{DA_n} m_{DA_n}}{-\omega^2 m_{DA_n} + k_{DA_n}} \\ 0 & 1 \end{bmatrix} \quad (2)$$

$$\alpha^{DV_n} = \begin{bmatrix} 1 & 0 \\ \frac{1}{-j\omega m_{DV_n}} & 1 \end{bmatrix} \quad (3)$$

It should be noted that the transmission matrix for the DVA describes a drive-point response. Hysteretic damping is included in the DVAs by using a complex stiffness $k_{DA_n}(1 - j\eta_{DA_n})$. The transmission matrix for the n^{th} resilient element modelled as a slender rod undergoing longitudinal vibration is given by (Dylejko et al., 2007):

$$\alpha^{RD_n} = \begin{bmatrix} \cos(k_l L_{RD_n}) & \frac{-AE k_l \sin(k_l L_{RD_n})}{-j\omega} \\ \frac{-j\omega \sin(k_l L_{RD_n})}{AE k_l} & \cos(k_l L_{RD_n}) \end{bmatrix} \quad (4)$$

$k_l = \omega/c_l$ is the longitudinal wavenumber and $c_l = \sqrt{E/\rho}$ is the longitudinal wave speed. Hysteretic damping is included by using a complex Young's modulus $E(1 - j\eta)$.

Coupled response

The transmission matrices of the individual stages can be calculated from:

$$\alpha^1 = \alpha^{M_0} \alpha^{RD_1} \parallel \alpha^{DV_1} \quad (5)$$

$$\alpha^2 = \alpha^{M_1} \alpha^{DA_1} \alpha^{RD_2} \parallel \alpha^{DV_2} \quad (6)$$

$$\alpha^3 = \alpha^{M_2} \alpha^{DA_2} \alpha^{RD_3} \quad (7)$$

Elements in series are combined by forward matrix multiplication. The symbol \parallel , represents an operation for adding transmission matrices in parallel and is described by (Snowdon, 1971):

$$\alpha' \parallel \alpha'' = \begin{bmatrix} A/B & (AC - B^2)/B \\ 1/B & C/B \end{bmatrix} \quad (8)$$

where

$$A = \sum_{i=1}^n \alpha_{11}^i / \alpha_{21}^i \quad (9)$$

$$B = \sum_{i=1}^n 1 / \alpha_{21}^i \quad (10)$$

$$C = \sum_{i=1}^n \alpha_{22}^i / \alpha_{21}^i \quad (11)$$

The subscripts of α^i refer to the row and column element number respectively of the transmission matrix α^i . The description of the complete system is given by:

$$\beta = \alpha^1 \alpha^2 \alpha^3 \quad (12)$$

The transmitted force can be calculated from (Snowdon, 1971):

$$f_e = (\beta_{11} + \beta_{12}/Z_d)^{-1} \quad (13)$$

Where β_{11} and β_{21} represent the first and second elements in the first row of the matrix β . Z_d is the drive-point impedance of the foundation; in this work, a rigid termination is assumed. The force transmissibility assuming $f_0 = 1$ is then defined as:

$$T_F = 20 \log_{10} |f_e| \text{ (dB)} \quad (14)$$

OPTIMISATION

Design parameters

The design parameters to be optimised for this work are the locations of the intermediate masses, properties of the DAVIs and the properties of the DVAs. Vectors including these design variables are respectively defined by:

$$\mathbf{x}^{\text{DM}} = \{ x_1 \quad x_2 \} \quad (15)$$

$$\mathbf{x}^{\text{DV}} = \{ m_{\text{DV}_1} \quad m_{\text{DV}_2} \} \quad (16)$$

$$\mathbf{x}^{\text{DA}} = \left\{ m_{\text{DA}_1} \quad \eta_{\text{DA}_1} \quad f_{\text{DA}_1} \quad \dots \right. \\ \left. m_{\text{DA}_2} \quad \eta_{\text{DA}_2} \quad f_{\text{DA}_2} \right\} \quad (17)$$

Where f_{DA_1} and f_{DA_2} are the DVA tuning frequencies. For the n^{th} DVA, the tuning frequency is related to the DVA mass and stiffness by: $f_{\text{DA}_n} = \sqrt{k_{\text{DA}_n}^r / m_{\text{DA}_n}}$, $k_{\text{DA}_n}^r$ is the real part of the complex stiffness k_{DA_n} . The design parameters can be combined to give:

$$\mathbf{x} = \left\{ \mathbf{x}^{\text{DM}} \quad \mathbf{x}^{\text{DV}} \quad \mathbf{x}^{\text{DA}} \right\} \quad (18)$$

Performance criteria

The primary performance criterion chosen for this work is the difference between the force transmissibility of a particular isolator configuration and an ideal isolator. This can be expressed by a relative force transmissibility which is a function of the design parameters and frequency:

$$T_{FR}(\mathbf{x}, \omega) = T_F(\mathbf{x}, \omega) - T_{FI}(\omega) \quad (19)$$

T_{FI} is the force transmissibility of an ideal isolator. The ideal isolator is modelled by replacing the resilient elements, otherwise described by Equation (4), with a stiffness of AE/L . The cost function to be minimised is the maximum relative force transmissibility over a chosen frequency range:

$$J(\mathbf{x}) = \max_{\omega_l \leq \omega_i \leq \omega_u} T_{FR}(\mathbf{x}, \omega_i) \quad (20)$$

ω_l and ω_u are the lower and upper frequency limits to be considered during the optimisation. This is the minimax problem. Another performance criterion for assessing the broadband response is the RMS transmissibility; this is defined as:

$$T_{F,RMS} = 10 \log_{10} \left(\sum_{\omega_i=\omega_l}^{\omega_u} 2 \times |f_e(\mathbf{x}, \omega_i)|^2 \times \Delta f \right) \text{ (dB)} \quad (21)$$

Δf is the frequency spacing at which the force transmissibility is evaluated. This parameter gives an estimate of the RMS transmitted force for a unity broadband excitation over the chosen frequency range.

Two configurations of isolator are considered in this paper. The first, is the configuration used by Du et al. (2005) which includes the two intermediate masses with the two DVAs. The cost function to be minimised becomes:

$$J(\mathbf{x}^{\text{DM}}, \mathbf{x}^{\text{DV}} = 0, \mathbf{x}^{\text{DA}}) \quad (22)$$

The second configuration includes the two intermediate masses with two DAVIs. The cost function in this case becomes:

$$J(\mathbf{x}^{\text{DM}}, \mathbf{x}^{\text{DV}}, \mathbf{x}^{\text{DA}} = 0) \quad (23)$$

These two configurations, one with DVAs and one with DAVIs, will be referred to as the DVA and DAVI isolators respectively.

Algorithm

Complex cost functions such as Equation (20) can include many local minima. Stochastic methods such as genetic algorithms, simulated annealing and particle swarm optimisation attempt to improve the chances of finding the global optimum. Often, this is achieved at the expense of computational efficiency. These global optimisation techniques do not require assumptions based on continuity or the existence of derivatives. For these reasons, they are well suited to minimise cost functions derived from models characterised by numerical or experimental methods.

For this work, a combination of a particle swarm algorithm (Kennedy and Eberhart, 1995) and a general non-linear constrained algorithm has been chosen. The particle swarm algorithm was chosen for its flexibility, simplicity and efficiency with large dimensional problems. While equality constraints may be included in the system model, inequality cannot be directly enforced by this algorithm. Constraints are included by shifting agents which violate the parameter constraints back to the edge of the search space. The general non-linear constrained algorithm is based on the sequential quadratic programming method (Nocedal and Wright, 1999). This algorithm is used to efficiently locate the minimum close to the final point of the search conducted by the particle swarm optimisation.

RESULTS

Numerical study

The values for the isolator parameters have been chosen to be consistent with the work completed by Du et al. (2003). The parameters not involved in the optimisation are presented in Table 1. It should be noted that the primary mass (m_0) has been reduced by a factor of three. This is to take into account the three isolators in parallel used by Du et al. (2003). It should also be kept in mind when comparing results from this work with Du et al. (2003) that the primary mass in their paper had multiple degrees-of-freedom and was supported on top of a flexible plate.

Table 1. Constant parameter values.

Parameter	Value
m_0 (kg)	9.27
m_1, m_2 (kg)	0.050
E (Pa)	20×10^6
ρ (kg/m ³)	1103
L (m)	0.066
A (m ²)	0.00123
η	0.1

The limits imposed on the design variables for the optimisation are given in Table 2.

Table 2. Optimisation limits.

Parameter		Lower limit	Upper limit
x_1	(m)	0.033	0.066
x_2	(m)	0	0.033
m_{DV}	(kg)	0	0.500
m_{DA}	(kg)	0	0.150
η_{DA}		0	0.4
f_{DA}	(Hz)	350	1200
f	(Hz)	200	3000

Optimum DVA isolator

The optimum parameters for the DVA isolator, found from minimising the cost function described by Equation (22) are given in Table 3. The cost function was evaluated numerically over the 200 Hz to 3000 Hz frequency range with a resolution of 1 Hz. The intermediate masses in the isolator presented by Du et al. (2003) were positioned at $x_1 = 0.0495$ m and $x_2 = 0.0165$. These locations were chosen based on practical considerations and a modal analysis of an isolator without intermediate masses. The optimum values found in this study are closer to the anti-nodes of the first two internal resonances for an isolator without intermediate masses (Du et al., 2003). Also different, is that the optimum DVA masses were not found to be the maximum allowable. Similar to their findings, however, the optimum loss factor for both DVAs was found to be the maximum value.

Table 3. Optimum parameters for DVA isolator.

Parameter		Value
x_1	(m)	0.052
x_2	(m)	0.031
m_{DA_1}	(kg)	0.068
η_{DA_1}		0.400
f_{DA_1}	(Hz)	753
m_{DA_2}	(kg)	0.133
η_{DA_2}		0.400
f_{DA_2}	(Hz)	350

The force transmissibility using a massless isolator (ideal); isolator including internal resonances (realistic); isolator including internal resonances and intermediate masses (compound) and the optimum DVA isolator is shown in Figure 4. The vertical dotted grey lines represent the frequency range considered during the optimisation. The rigid body resonance (f_0) of the primary mass can be observed at a frequency of 32 Hz. For the ideal isolator, the transmissibility drops below 0 dB after $\sqrt{2}f_0$ and then decreases at a rate of approximately 12 dB per octave. The internal resonances occur at 1020 Hz, 2090 Hz and 3060 Hz for the frequency range displayed. The inclusion of the internal resonances in the realistic isolator decreases the performance of the isolator compared with the ideal isolator by up to 26 dB. The rate at which the transmissibility

drops with frequency is reduced to around 6 dB per octave. The inclusion of the intermediate masses in the compound isolator lowers the first two resonances to 625 Hz and 1196 Hz. The rate at which the transmissibility decays at frequencies above these two intermediate mass resonances is increased. This phenomena is exploited in multi-stage vibration isolation systems (Moore, 2011).

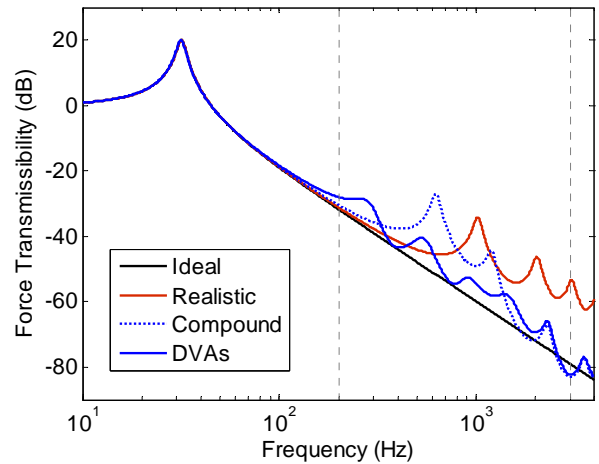


Figure 4. Force transmissibility for an ideal, realistic, compound and optimum DVA isolator.

The optimum DVA isolator reduces the maximum difference in transmissibility relative to the ideal isolator to 8.5 dB. This is a 17.5 dB improvement over the realistic isolator. Also, the transmissibility roll-off with frequency is similar to that of the ideal isolator. The RMS transmissibility, however, has increased from -5.9 dB to -4.8 dB compared with the realistic isolator. This is due to the increase in transmissibility at lower frequencies. Although not shown, an interesting observation was that the internal resonances had little influence over the motion of the primary mass. This implies that the primary mass is de-coupled at these higher frequencies. Unlike the optimum DVA isolator presented by Du et al. (2003), the highest DVA tuning frequency is not close to the first resonance of the compound isolator. This suggests that the traditional method of tuning a DVA to a problem resonance is not suitable for best performance with the chosen cost function. Previous research with DVAs has also demonstrated the benefits of a detuned strategy (Fuller et al., 1997).

Optimum DAVI isolator

The optimum parameters for the DAVI isolator found from minimising the cost function described by Equation (23) are given in Table 4.

Table 4. Optimum parameters for DAVI isolator.

Parameter		Value
x_1	(m)	0.034
x_2	(m)	0.013
m_{DV_1}	(kg)	0.110
m_{DV_2}	(kg)	0.040

The cost function was again evaluated numerically over the 200 Hz to 3000 Hz frequency range with a resolution of 1 Hz. Interestingly, the optimum locations of the two interme-

diate masses are quite different from the DVA isolator. For the DAVI, the intermediate masses are roughly in the centre and 1/5th of the length from the bottom. These locations are also close to anti-nodes of the first two internal resonances for an isolator without the intermediate masses (Du et al., 2003). The force transmissibility with a massless isolator (ideal); isolator including internal resonances (realistic); isolator including internal resonances and intermediate masses (compound) and the optimum DAVI isolator is shown in Figure 5.

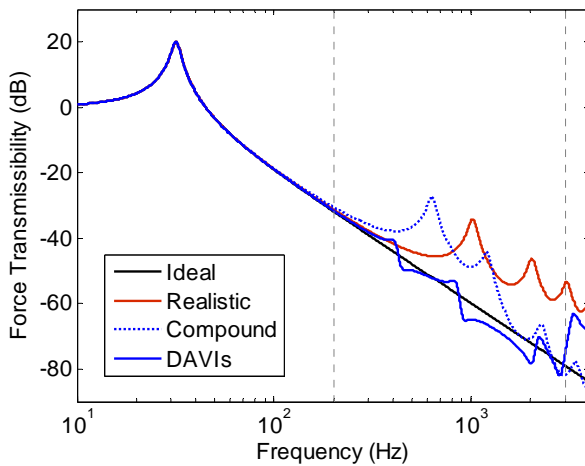


Figure 5. Force transmissibility for an ideal, realistic, compound and optimum DAVI isolator.

Even though the locations of the intermediate masses are different to those of the DVA isolator, the compound isolator transmissibility for both configurations is very similar. This is explained by the symmetry of the intermediate mass locations about the centre of the isolator for the two different configurations. With the introduction of the optimum DAVIs, the maximum deviation in force transmissibility relative to the ideal isolator over the chosen frequency range is reduced to 3.6 dB. This represents a 22.4 dB improvement over the realistic isolator. An interesting feature in the transmissibility is the wide suppression band established between 867 Hz and 2143 Hz where the transmissibility drops below the ideal case. Also of interest, are the two anti-resonances occurring within this frequency band. Similar to the optimum DVA, the transmissibility roll-off in frequency over the chosen bandwidth is close to the ideal case. Above 3 kHz, however, the response increases to levels similar to the realistic isolator. This is due to the inertial coupling associated with the DAVIs which negates the increase in frequency roll-off of normally associated with the intermediate masses. The RMS transmissibility has been reduced to -10 dB which is only 0.4 dB higher than the ideal case.

Sensitivity analysis

To understand the effect of manufacturing and material tolerances on the performance of real isolators, it is necessary to conduct a sensitivity analysis. The most sensitive parameters for the DVA isolator taking into account J as the performance criterion were found to be the tuning frequencies of the DVAs (f_{DA_1} and f_{DA_2}). The DAVI isolator was more sensitive to changes in the locations of the intermediate masses (x_1 and x_2). These four parameters are plotted together in Figure 6 over a perturbed parameter range of $\pm 5\%$.

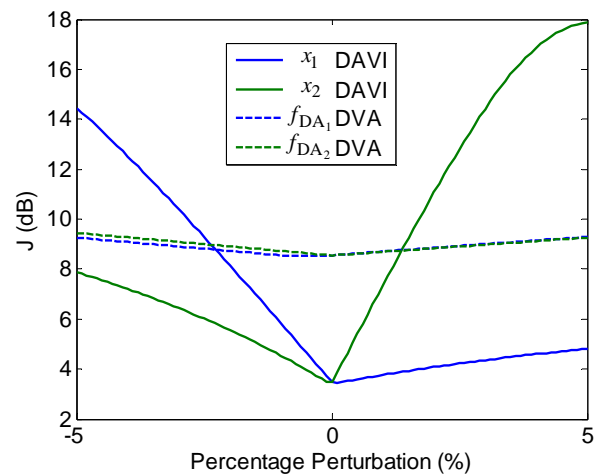


Figure 6. Effect of parameter perturbations on J .

The curves in Figure 6 were produced by perturbing a single parameter with the others remaining at their optimal value. It can be seen that the DAVI isolator is far more sensitive to parameter perturbations than the DVA isolator. This result shows that perhaps it would be preferable to suffer a slight loss in performance for a reduction in parameter sensitivity. This criterion could be included in the optimisation process. It was found that the RMS transmissibility, however, was far less sensitive to changes in the design parameters.

A perturbation analysis was also carried out. All the combinations of -5%, 0% and +5% variations in the design parameters were evaluated against J to find the worst case. The worst case perturbations for the DVA and DAVI isolators are listed in and Table 5 and Table 6 respectively. The force transmissibilities for the worst case DVA and DAVI isolators are shown against the optimum responses in Figure 7 and Figure 8 respectively. The worst case DVA isolator incurs an increase in J from 8.5 dB to 11 dB. The RMS transmissibility for this parameter set changes from -4.8 dB to -5 dB. The DAVI isolator suffers a large increase in J from 3.6 dB to 18.6 dB. Examining Figure 8 shows that this is due to a resonance shifting into the frequency range considered in the calculation of J . The RMS transmissibility, however, remains unchanged. This is due to a wide suppression band being established which covers lower frequencies.

Table 5. Worst case perturbations for DVA isolator.

x_1	x_2	m_{DA_1}	η_{DA_1}	f_{DA_1}	m_{DA_2}	η_{DA_2}	f_{DA_2}
-5%	+5%	-5%	-5%	+5%	-5%	-5%	-5%

Table 6. Worst case perturbations for DAVI isolator.

x_1	x_2	m_{DV_1}	m_{DV_2}
-5%	+5%	+5%	+5%

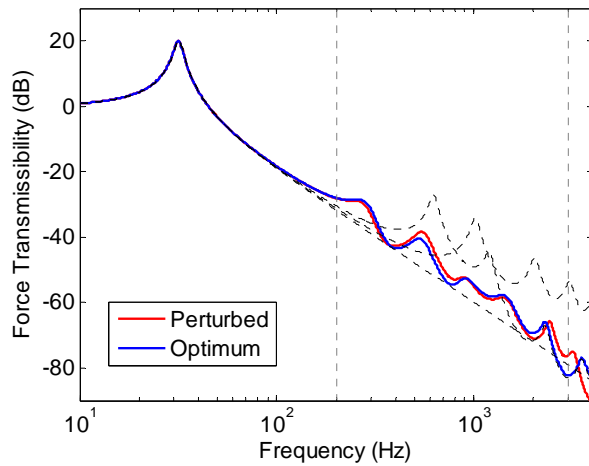


Figure 7. Force transmissibility of perturbed and optimum DVA isolator.

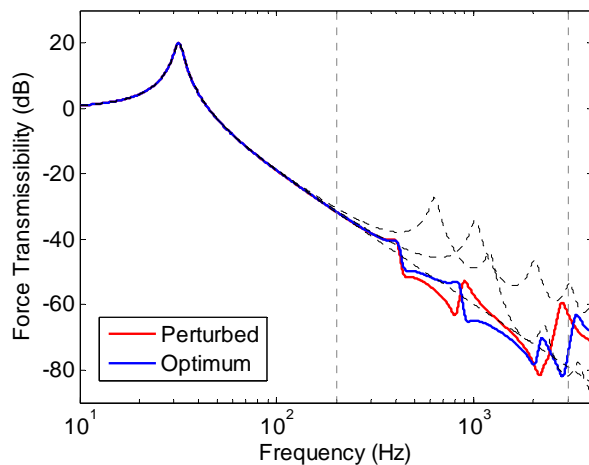


Figure 8. Force transmissibility of perturbed and optimum DAVI isolator.

Summary of results

A summary of the performance criteria evaluated for the different isolator configurations is presented in Table 7.

Table 7. Summary of the performance of the different isolator configurations.

Isolator	J (dB)	$T_{F,RMS}$ (dB)
Ideal	0	-10.4
Realistic	26.0	-5.9
DVA	8.5	-4.8
DAVI	3.6	-10.0
Perturbed DVA	11.0	-5.0
Perturbed DAVI	18.6	-10.0

CONCLUSIONS

This paper is a preliminary theoretical study into the use of an inertial mechanism within a uni-axial vibration isolator for suppressing the influence of internal resonances on force transmission. The inertial mechanism under consideration is a device that exerts an inertial force proportional to the relative acceleration of its connection points.

Two isolator configurations were examined. The first was a compound vibration isolator incorporating dynamic vibration absorbers, referred to as the DVA isolator. This design was proposed by Du et al. (2003). The second, referred to as the DAVI isolator, was a concept that incorporated ideal inertial mechanisms coupling the primary mass to the intermediate masses. The design parameters under consideration were the intermediate mass locations; dynamic vibration absorber properties and the effective masses of the inertial mechanisms.

The force transmissibility of the isolators supporting a primary mass was modelled analytically using the transmission matrix approach. This allows for greater flexibility for future design changes. The primary mass, intermediate masses, dynamic vibration absorbers and inertial mechanism were considered as lumped parameters. The resilient elements were modelled as continuous slender rods undergoing longitudinal vibration. This approximation has been shown previously to compare well with experimental results (Harrison et al., 1952). The elastic response of the inertial mechanism was not considered in this preliminary study.

A cost function was defined as the maximum deviation in force transmissibility from an ideal isolator. Optimum design parameters were found for the two isolator configurations by minimising this cost function over a chosen frequency range. Realistic constraints were imposed on the parameters during this optimisation. A particle swarm and gradient based algorithm was used to find the global optima. It was shown that for the chosen frequency range, both isolator configurations significantly reduced the influence of the internal resonances on the force transmissibility. The DVA configuration reduced the maximum difference in force transmissibility from an ideal isolator by 17.5 dB. The DAVI isolator configuration improved on this result with a reduction of 22.4 dB. This configuration was found to have an RMS force transmissibility close to that of an ideal isolator. This represents a 5.2 dB improvement in RMS transmissibility over the DVA isolator.

Finally, a sensitivity and perturbation analysis was performed to assess the impact of variations in design parameters. It was found that the DAVI isolator was more sensitive to changes in the design parameters than the DVA isolator. The results demonstrate, however, that a small compromise in maximum force transmissibility relative to an ideal isolator could be made to reduce this sensitivity.

ACKNOWLEDGEMENTS

The author would like to thank Stephen Moore for his useful suggestions and Kathryn Ackland for an elegant solution which improved the efficiency of the perturbation analysis.

REFERENCES

- Beranek, LL & Vér, IL (Eds.) 1992, *Noise and Vibration Control Engineering Principles and Applications*, New York, John Wiley & Sons, Inc.
- Desjardins, RA & Hooper, EW 1978, 'Helicopter rotor vibration isolation', *Vertica*, vol. 2, pp. 145-159.
- Dickens, JD 1999, *Investigation of asymmetrical vibration isolators for maritime machinery applications*, DSTO-RR-0168, Defence Science and Technology Organisation.
- Du, Y, Burdisso, RA & Nikolaidis, E 2005, 'Control of internal resonances in vibration isolators using passive and hybrid dynamic vibration absorbers', *Journal of Sound and Vibration*, vol. 286, pp. 697-727.
- Du, Y, Burdisso, RA, Nikolaidis, E & Tiwari, D 2003, 'Effects of isolators internal resonances on force transmissibility and radiated noise', *Journal of Sound and Vibration*, vol. 268, pp. 751-778.
- Dylejko, PG, Kessissoglou, NJ, Tso, Y & Norwood, CJ 2007, 'Optimisation of a resonance changer to minimise the vibration transmission in marine vessels', *Journal of Sound and Vibration*, vol. 300, pp. 101-116.
- Flannelly, WG 1967, *Dynamic antiresonant vibration isolator*, United States of America patent application, no. 3,322,379.
- Fuller, CR, Maillard, JP, Mercadal, M & Von Flotow, AH 1997, 'Control of aircraft interior noise using globally detuned vibration absorbers', *Journal of Sound and Vibration*, vol. 203, pp. 745-761.
- Harris, CM (Ed.) 1995, *Shock and Vibration Handbook*, New York, McGraw-Hill.
- Harrison, M, Sykes, AO & Martin, M 1952, 'Wave effects in isolation mounts', *The Journal of the Acoustical Society of America*, vol. 24, pp. 62-71.
- Kennedy, J & Eberhart, R 1995, 'Particle swarm optimization', *Proceedings of IEEE International Conference on Neural Networks*, Piscataway, NJ.
- Mcguire, DP 2003, 'High stiffness ("rigid") helicopter pylon vibration isolation systems', *American Helicopter Society 59th Annual Forum*, Phoenix, Arizona.
- Moore, S 2011, 'Analytical modelling of single and two-stage vibration isolation systems', *Proceedings of Acoustics 2011*, Australian Acoustical Society, Gold Coast, Australia.
- Nocedal, J & Wright, S 1999, *Numerical optimization*, New York, Springer-Verlag.
- Rubin, S 1967, 'Mechanical immittance- and transmission-matrix concepts', *The Journal of the Acoustical Society of America*, vol. 41, pp. 1171-1179.
- Smith, MC 2002, 'Synthesis of mechanical networks: The inerter', *IEEE Transactions on Automatic Control*, vol. 47, pp. 1648-1662.
- Smith, RS, Pascal, RJ, Lee, T, Stamps, BF, Van Schoor, M C, Masters, BP, Blaurock, C, Prechtl, EF, Rodgers, JP & Merkley, DJ 2002, 'Results from the dynamically tailored airframe structures program', *American Helicopter Society 58th Annual Forum*, Montréal, Canada.
- Snowdon, JC 1971, 'Mechanical four-pole parameters and their application', *Journal of Sound and Vibration*, vol. 15, pp. 307-323.
- Snowdon, JC 1979, 'Vibration isolation: Use and characterization', *The Journal of the Acoustical Society of America*, vol. 66, pp. 1245-1274.
- Sykes, AO 1960, 'Isolation of vibration when machine and foundation are resilient and wave effects occur in the mount', *Noise Control*, vol. 6, pp. 23-27 and 30-38.
- Yan, B, Brennan, MJ, Elliott, SJ & Ferguson, NS 2010, 'Active vibration isolation of a system with a distributed parameter isolator using absolute velocity feedback control', *Journal of Sound and Vibration*, vol. 329, pp. 1601-1614.
- Yilmaz, C & Hulbert, GM 2010, 'Theory of phononic gaps induced by inertial amplification in finite structures', *Physics Letters A*, vol. 374, pp. 3576-3584.
- Yilmaz, C & Kikuchi, N 2005, 'Analysis and design of passive band-stop filter-type vibration isolators for low-frequency applications', *Journal of Sound and Vibration*, vol. 291, pp. 1004-1028.